JOURNAL OF SOLID STATE CHEMISTRY 115, 146–151 (1995)

Synthesis and Magnetic and Electrical Properties of the Molybdenum and Tungsten Pyrophosphates MP_2O_7 (M = Mo, W)

L. Lezama, J. M. Rojo, J. L. Mesa, and T. Rojo[1]

Departamento de Química Inorgánica, Facultad de Ciencias, Universidad del País Vasco, Apdo. 644, E-48080 Bilbao, Spain

and

R. Olazcuaga

Laboratoire de Chimie du Solide du CNRS, Université de Bordeaux I, 351 Cours de la Liberation, 33405 Talence Cedex, France

Received April 18, 1994; in revised form July 7, 1994; accepted July 13, 1994

The molybdenum and tungsten pyrophosphates MP_2O_7 (M = Mo, W) have been synthesized and characterized. The structure of these isostructural compounds is built up from $|MO_6|$ (M = Mo, W) octahedra sharing their corners with P_2O_7 groups. These polyhedra are in mixed layers characterized by pentagonal windows which delimit intersecting zigzag tunnels. The measured conductivity for these compounds is in agreement with the behavior of "hopping semiconductors." The magnetic behavior indicates both a large zero-field splitting and the existence of antiferromagnetic interactions with a marked 3D character.

INTRODUCTION

The great ability of the phosphate frameworks to stabilize reduced oxidation states of molybdenum and tungsten has been pointed out during the past decade. These materials exhibit interesting properties with potential applications, especially in heterogeneous catalysis, ionic exchange, and electron transport (1, 2). The interest of these phases is increased by the high degree of mechanical, chemical, and thermal stability provided by the $|PO_4|$ groups. Moreover, in spite of their similar electronic configurations, molybdenum and tungsten compounds can exhibit very different behavior.

Tungsten is characterized by its ability to form W(V)–W(VI) mixed valency phosphates (3). In these compounds very anisotropic metallic or semimetallic properties have been observed and these compounds are called bronzes. In fact, these materials are strongly related to the famous tungsten bronzes A_xWO_3 (discovered by Magnéli in 1953 (4)). The octahedral frameworks over which the conducting electrons are generally delocalized in the Magnéli phases are preserved in part in the phosphate tungsten bronzes, due to the adaptability of the $|PO_4|$ tetrahedra and $|P_2O_7|$ groups to the octahedral framework. The great number of possible ways of connecting the pyrophosphate group, which possesses height similar to that of $|WO_6|$ and great flexibility due to the free rotation of the two $|PO_4|$ tetrahedra with respect to each other, is remarkable.

Most of the studied phosphate tungsten bronzes can be included in one of the following families (3): (a) diphosphate tungsten bronzes with hexagonal tunnels, $DPTB_H$, with the general formula $A_x(P_2O_4)_2(WO_3)_{2m}$; (b) monophosphate tungsten bronzes with pentagonal tunnels, $MPTB_P$, with the general formula $(PO_2)_4(WO_3)_{2m}$; (c) monophosphate tungsten bronzes with hexagonal tunnels, $MPTB_H$, with the general formula $A_x(PO_2)_4(WO_3)_{2m}$; (d) diphosphate tungsten bronzes with hexagonal tunnels, $DPTB_H$, with the general formula $(P_2O_4)_2(WO_3)_{2m}$, m being an integral number commonly between 4 and 20. The difficulty in isolating these compounds as pure phases increases with the value of m.

On the other hand, molybdenum, owing to its numerous possible oxidation states (VI, V, IV, III), is a potential candidate for the formation of mixed valency materials. However, as yet, in the mixed frameworks of octahedral molybdenum phosphates, only Mo(IV)–Mo(III) compounds have been observed (5–8). Among these compounds, one of the most interesting is the molybdenum(IV) pyrophosphate (9, 10). This compound exhibits a ZrP_2O_7 type structure (11), characterized by the presence of pentagonal tunnels. This structural type is also characterized by its ability to accommodate tetravalent cations with ionic radii widespread from Si^{4+} (0.40 Å) to Th^{4+} (1 Å), with a linear increase in the unit-cell parameter with the ionic radius. Taking into account that due to the lanthanide contraction, the ionic radii of Mo(IV) and W(IV) are practically the same (0.65 Å) (12),

[1] To whom all correspondence should be addressed.

0022-4596/95 $6.00

the obtention of a tungsten (IV) pyrophosphate appeared to be possible. As a result, Teweldemedhin *et al.* (13) have recently published the synthesis of the WP_2O_7 compound.

As a part of our investigation on molybdenum phosphates, we have found a synthetic pathway that leads to the obtention of the MoP_2O_7 pyrophosphate as a pure phase. Using this procedure for the W–P–O system we have also been able to prepare the WP_2O_7 compound. The present work deals with the synthesis, structural characterization, magnetic behavior, and electron transport properties of these materials.

EXPERIMENTAL

Preparation of the MP_2O_7 (M = Mo, W) Compounds

The starting materials were mixtures of MoO_3 or WO_3 oxides and $(NH_4)_2HPO_4$, with the molar ratio of $1M:5P$, (M = Mo or W). The mixtures were ground and put into an alumina crucible. Calcination was carried out in air by using an electrical furnace at two sequential temperatures. At first temperature, about 250°C, the ammonium phosphate decomposed, and then the samples reacted at 600°C for 4 hr. The dark products obtained, recovered microcrystalline powder compounds, which correspond to MoP_2O_7 and WP_2O_7 stoichiometries, were dissolved in hot water.

Molybdenum, tungsten, and phosphorus content were confirmed by atomic absorption (Perkin–Elmer 3030B) and gravimetric techniques, respectively. The results were as follows: found: Mo, 35.3% (W, 51.1%); P, 22.9 (17.0); required: Mo, 35.5 (W, 51.4); P, 23.0 (17.3).

X-Ray Crystallography

A STOE automatic powder diffraction system, operating at 40 kV, 20 mA, with monochromatic Cu$K\alpha_1$ radiation (1.5406 Å), has been used to record the X-ray powder diffraction patterns of the compounds. A scan ω-2θ has been performed, with steps of 0.02° in 2θ and a fixed-time counting of 15 sec. Room temperature was maintained at 298(1) K.

Physical Measurements

IR spectra (KBr pellet) were obtained with a Nicolet FT-IR 740 spectrophotometer. Magnetic susceptibility measurements were performed on a polycrystalline sample using a DSM8 magnetometer/susceptometer between 4.2 and 300 K. A Bruker ESP300 spectrometer, operating at X and Q bands, was used to study the ESR polycrystalline spectra between 4.2 and 300 K. The temperature was stabilized by an Oxford Instrument (ITC4) regulator. The magnetic field was measured with a Bruker 200 gaussmeter, and the frequency inside the cavity was determined using a Hewlett–Packard 5352B microwave frequency counter. The conductivity was measured by the four-point method (14). It was calculated by measuring the intensity/voltage ratio between the points in both directions of the current in order to minimize the dissymmetry effect between the contacts.

RESULTS AND DISCUSSION

The X-ray powder diffraction patterns of both molybdenum and tungsten pyrophosphate compounds are similar (Fig. 1). They have been indexed using the LSUCRE program (15) in a cubic unit-cell with the $Pa3$ space group, previously determined by Leclaire *et al.* (10) for the MoP_2O_7 compound, from the X-ray single crystal data. From Table 1, it can be seen that the unit-cell dimensions of these compounds are similar, and correspond to two cations, molybdenum and tungsten, belonging to the second and third series of transition metals, respectively. The calculated density for WP_2O_7, 4.74 g cm^{-3}, is in agreement with the measured value, 4.73(1) g cm^{-3}, obtained by the hydrostatic method.

The structure of the MoP_2O_7 compound was described by Leclaire *et al.* (10) as a three-dimensional framework built up from $|MoO_6|$ octahedra sharing their corners with

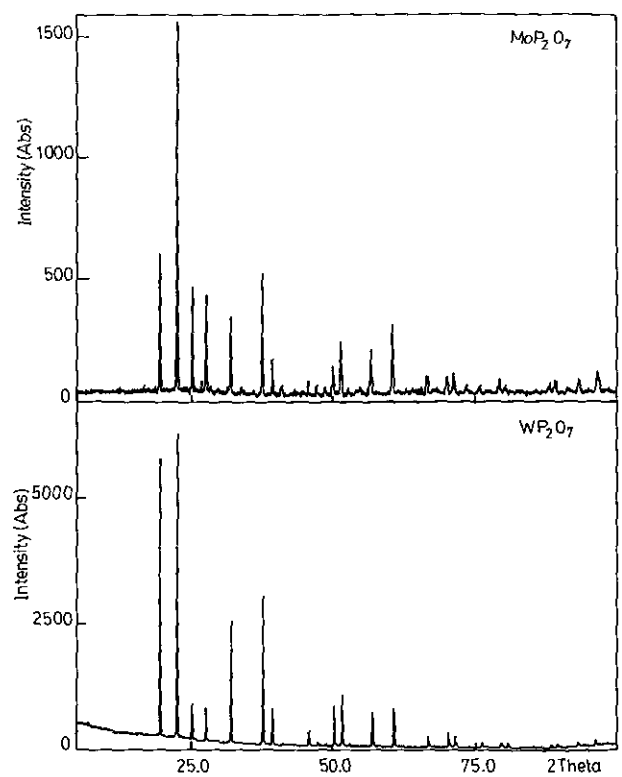

FIG. 1. X-ray powder diffraction patterns of the MP_2O_7 (M = Mo, W) compounds.

TABLE 1
Unit-cell Dimensions of the MP_2O_7 (M = Mo, W) Compounds

Compound	a (Å)	V (Å^3)	Z	ρ_{exp} (g cm^{-3})	r_{calc} (g cm^{-3})
MoP_2O_7	7.944(1)[a]	501.4(2)[a]	4[a]	3.53[b]	3.57[b]
WP_2O_7	7.942(1)	500.9(2)	4	4.73(1)	4.74

[a,b] From Refs. (10) and (9), respectively.

$[P_2O_7]$ groups. Thus the octahedra are completely surrounded by the pyrophosphate anions (see Fig. 2). These polyhedra give mixed layers characterized by the presence of pentagonal windows limited by two octahedra and three tetrahedra. The layers are staggered in such a way that the pentagonal windows delimit intersecting zigzag tunnels. Likewise, it can be observed the classical geometry of the diphosphate group, with three short P–O bonds [1.42(3) Å] corresponding to the oxygen atoms common to tungsten and phosphorus atoms, and a longer one [1.510(9) Å] corresponding to the oxygen atom bridging two phosphorus atoms.

Over the past years, the real structure of zirconium and molybdenum pyrophosphate compounds has not been completely determined. In 1971, Chaunac (16) reported that under most preparative conditions ZrP_2O_7 has a weak superstructure. Recently, Haushalter and Mundi (1) have observed in the MoP_2O_7 compound, with the aid of synchroton radiation, a few weak reflections belonging to a superstructure, which suggest an orthorhombic symmetry. Unfortunately, the superstructure of these pyrophosphate compounds has not yet been resolved. However, these crystallographic results have not precluded carrying out a study of the physical properties of these MP_2O_7 (M = Mo, W) compounds.

IR spectroscopy is a useful technique for the identification of different types of phosphates. Good correlations between the essential vibrational features and the structural data can be obtained (17, 18). However, for phosphates containing high-oxidation-state cations, the cation–oxygen force is large enough to alter the P–O vibrational frequency, and additional information may be needed. For the condensed phosphates, due to the existence of two types of P–O bonds, an additional approximation could be considered. The P–O_{ext} distance, for an "external" oxygen, is shorter than for an "internal" or bridging one within the P–O–P chain or ring, and the stretching frequency is accordingly higher.

The IR bands of the molybdenum and tungsten pyrophosphates are shown and compared with other pyrophosphates of transition elements in Table 2 (19). Band assignments have been empirically made on the basis of those reported by Rulmont *et al.* (18) and Huang *et al.* (19) for the pyrophosphates given in the literature. The spectra are complex, but in general three characteristic groups of bands are observed in the range 1300–700 cm^{-1}. Two broad bands approximately centered at 1230 and 1100 cm^{-1} for the MoP_2O_7 and three bands at 1260, 1160, and 1000 cm^{-1} for the WP_2O_7 are observed. These bands correspond to the ν_{as}(P–O_{ext}) antisymmetric stretch of the pyrophosphate groups. The bands ascribed to the antisymmetric stretch of the P–O–P bridge appear around 960 and 930 cm^{-1} for the molybdenum and tung-

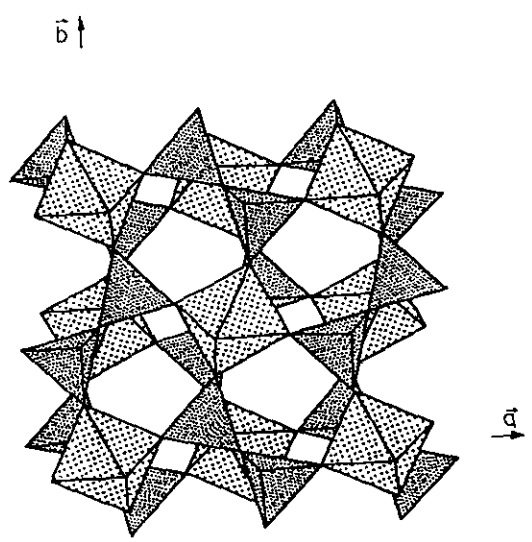

FIG. 2. Schematic illustration of the structure of the MoP_2O_7 compound.

TABLE 2
Selected IR Bands (cm^{-1}) and Empirical Assignments for Several MP_2O_7 Pyrophosphates of Transition Elements between 400 and 1500 cm^{-1}

Assignment	Ti[a]	Zr[a]	Mo	Hf[a]	W
	1280w	1270w	1230s		1260m
ν_{as} (P–O_{ext})	1095vs	1132vs	1100vs	1120vs	1160vs
				1051vs	1000s
ν_{as} (P–O_{int})	960s	981s	960s	962vs	930s
ν_s (P–O_{int})	741w	746w	740m	742m	740m
ν_{as} (M–O)	621m	690w			
&	583w	549s	525s	540s	530s
δ_{as} (O–P–O)	561m	500w			
δ_s (O–P–O)	448m			445w	
&			435m		430m
δ (O–M–O)		409w		409w	

Note. vs, very strong; s, strong; m, medium; w, weak.
[a] From ref. (19).

sten pyrophosphates, respectively. The more characteristic band of these types of compounds is due to the symmetric stretch of the P–O–P bridge, which appears at 740 cm^{-1} in both compounds. According to Lazarev's analysis (20), this vibration should be IR inactive if the anions were of symmetry D_{3d} or D_{3h}. Thus, its observation prevents the P–O–P bridge from being linear, as implied by the $Pa3$ space group determined by X-ray diffraction (Leclaire *et al.* (10)). This problem has also been found in other isotypic compounds (ZrP_2O_7, SnP_2O_7, SiP_2O_7) (19, 21, 22), and it is mainly associated with inexact location of the O(1) oxygen atom on the ternary axis.

The region of lower frequencies in the IR spectra is similar for both compounds. Two strong and broad bands, centered at 525 and 435 cm^{-1} for the molybdenum compound and 530 and 430 cm^{-1} for the tungsten compound, were observed. The band which appears at approximately 530 cm^{-1} has been observed in other pyrophosphates of tetravalent elements (Sn, Pb) (23) and can be assigned to the antisymmetric stretching modes in the $[MO_6]$ octahedra. The bands around 430 cm^{-1} are usually ascribed to the bending modes of the pyrophosphate groups which are strongly coupled with the vibrational modes of the $[MO_6]$ octahedra.

Magnetic susceptibility measurements were performed in the 4.2–300 K temperature range for both compounds (Fig. 3). No remarkable anomalies were detected on the susceptibility vs temperature curves, but the thermal dependence observed for the magnetic susceptibility of WP_2O_7 clearly contrasts with the Pauli paramagnetic behavior described for tungsten bronzes (24).

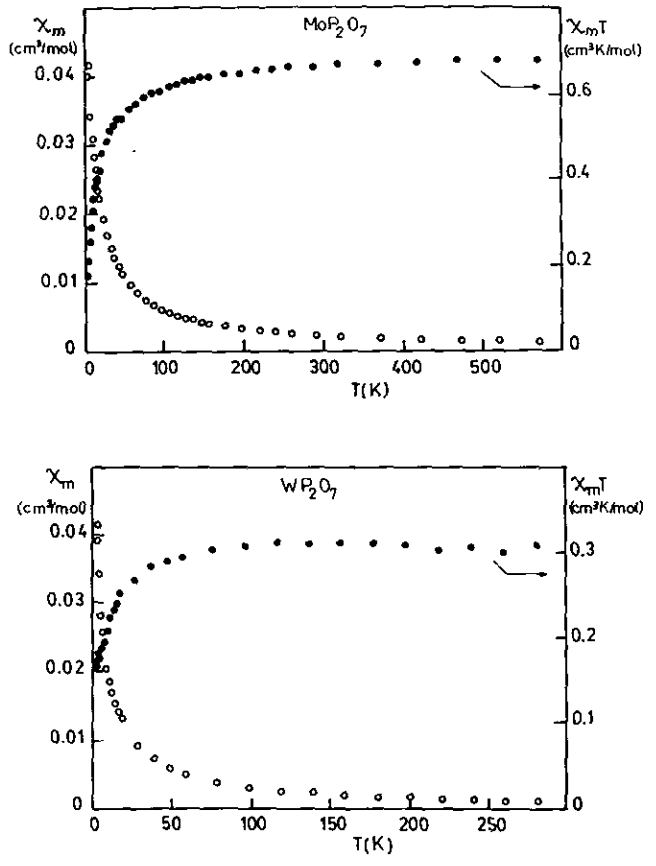

FIG. 3. Thermal evolution of the X_m and $X_m T$ for MP_2O_7 (M = Mo, W) compounds.

In both cases the data are well described by a Curie–Weiss law, with $C = 0.70$ cm^3K/mole, $\theta = -13.7$ K and $C = 0.31$ cm^3K/mole, $\theta = -4.2$ K for the molybdenum and tungsten pyrophosphates, respectively. In order to explain the extremely low value observed for the Curie constant of the tungsten compound, it is necessary to take into account the strong influence of the spin–orbit coupling in a $5d$ ion ($\lambda = 1050$ cm^{-1} for the W(IV) free ion (25)), which causes a strong reduction of the magnetic effective moment with respect to the "spin-only" magnetic moment. Considering the Russell–Saunders coupling scheme for tungsten, the expected magnetic moment of W(IV) is 1.63 μ_B (26) ($C = 0.33$ cm^3K/mol), in good agreement with the experimental data of WP_2O_7.

The effective magnetic moments decrease with decreasing temperature below 100 K, the molybdenum and tungsten phases respectively reach values of 1.26 and 1.16 μ_B at 4.2 K and values of 2.63 and 1.55 μ_B at room temperature. This fact, and the negative θ values, suggest that the main magnetic interactions in these compounds are antiferromagnetic.

However, for heavy transition metals this result must be cautiously evaluated due to the great importance of the spin–orbit coupling. This tends to cause energy level degeneracies to be resolved and it originates large splitting at zero-field and also gives rise to short spin-lattice relaxation times (27). For the last reason, ESR spectra of these types of compounds can only be observed at helium temperatures. Nevertheless, in our case no signal was detected in the ESR experiments even at 4.2 K, indicating the existence of rather strong zero-field splitting. Taking into account that the zero-field splitting of the isoelectronic V(III) ion is always positive (doublet above the singlet) in every case in which it has been evaluated (28), and extrapolating this situation to Mo(IV) and W(IV), decreasing temperature will cause depopulation into a diamagnetic ground state and therefore decrease the effective magnetic moment, an effect qualitatively similar to an antiferromagnetic interaction.

Using the Van Vleck equation, one can easily deduce an analytical expression for the susceptibility of anisotropically magnetic behavior, originating by the zero-field splitting, in the absence of any appreciable exchange. The resulting expression deviates appreciably from the Curie–Weiss law when $D/kT \rightarrow 1$. However, the experi-

mental χ^{-1} data follow straight lines in the whole range of measured temperature. Moreover, spin–orbit coupling increases with the atomic number, so that more important zero-field splitting is expected for W(IV) than for Mo(IV), but the θ value is greater for the MoP_2O_7 compound. Thus, the nonzero value of θ cannot only be ascribed to the effect of the zero-field splitting, and magnetic interactions must take place.

Considering the structural features exhibited by these pyrophosphates, antiferromagnetic interactions (with a marked 3D character) must be propagated by a superexchange mechanism through the $|P_2O_7|$ groups, as has been confirmed for other molybdenum phosphates (29, 30).

Measurements of electrical resistivities were performed from room temperature to 400°C. At higher temperatures the resistivity is about $10^5\ \Omega \cdot$ cm for both compounds, and it becomes greater than $10^8\ \Omega \cdot$ cm at 100°C. In Fig. 4 is represented the variation of conductivity as a function of temperature, showing the characteristics of semiconducting behaviors. Below 235 and 130°C for the molybdenum and tungsten pyrophosphates, respectively, the conductivity becomes too weak for our instrumentation and the data could not be accurately measured. The activation energy calculated for the high temperature region (250–400°C), was 0.85 and 0.81 eV for the molybdenum and tungsten compounds, respectively.

The observed conductivity values are much lower than those observed in other semiconductor compounds of the W–P–O system, e.g., for WPO_5, $\sigma \approx 10^2\ (\Omega \cdot \text{cm})^{-1}$ at room temperature with an activation energy of 0.084 eV (31), and obviously the values do not correspond to the metallic behavior expected for a tungsten bronze. These results and the localized magnetic moment suggest the presence of localized electrons. The observed electronic conductivity may be associated to a hopping phenomenon.

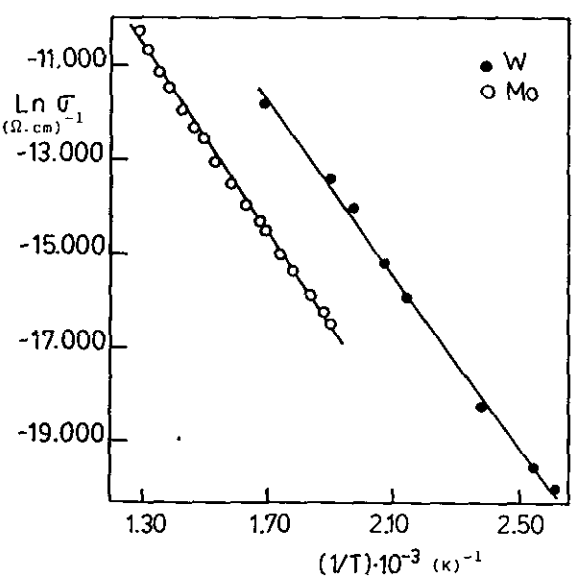

FIG. 4. Evolution of *Ln* conductivity (*Ln* σ) vs reciprocal temperature ($1/T$) for MP_2O_7 (M = Mo, W) compounds.

Reactions of molybdenum or tungsten pyrophosphates with sodium iodide from aqueous solution allow to obtain phases in which the sodium cation has been incorporated to the crystal structure. The study of these new phases by ESR spectroscopy indicates that Mo(III) or W(III) are also present. A more detailed study of these reactions is being carried out.

CONCLUDING REMARKS

Interest in these materials lies mainly in the presence of interconnected pentagonal tunnels. Due to these opened structures, they are able to accept small ions or molecules. There also exists the possibility of redox intercalation reactions occurring where the molybdenum/tungsten can be either reduced or oxidized, and could thus be used as ionic exchangers or catalysts. From this point of view the optimization of the synthetic pathways that can lead to pure phases is a very important startpoint, and as a result, it appears that the M/P ratio in the reaction medium is the most important parameter to consider. The considerable zero-field splitting presented in the studied compounds originating from the spin–orbit coupling, which also causes a strong reduction on the magnetic effective moment of the tungsten pyrophosphate, is remarkable. On the other hand, the temperature dependence of the magnetic susceptibility observed for WP_2O_7, as well as its electron transport properties, indicate that electronic delocalization is not present, at least below room temperature. Therefore, even if some structural features and the composition indicate that WP_2O_7 is the first member ($m = 1$) of the diphosphate tungsten bronzes with pentagonal tunnels ($DPTB_p$ $(P_2O_4)(WO_3)_{2m}$), the observed properties do not allow it to be considered a bronze. Although the $|PO_4|$ groups are effective in transmitting the magnetic interactions, the covalent character of the P–O bonds precludes their participation in electron conduction. For this reason, electronic localization is observed when the $|WO_6|$ octahedra are only linked to $|PO_4|$ tetrahedra, which occur in WP_2O_7, in contrast with the $|WO_6|$–$|WO_6|$ bonds present in the tungsten bronzes.

ACKNOWLEDGMENTS

This work was financially supported by Basque Country Government Grant PGV 9239 and DGICYT Grant PB90-0549 which we gratefully acknowledge.

REFERENCES

1. R. C. Haushalter and L. A. Mundi, *Chem. Mater.* **4**, 31 (1992).
2. A. Clearfield, *Chem. Rev.* **88**, 125 (1988).

3. M. M. Borel, M. Goreaud, A. Grandin, Ph. Labbé, A. Leclaire, and B. Raveau, *Eur. J. Solid State Inorg. Chem.* **28,** 93 (1991).
4. A. Magnéli, *Acta Chem. Scand.* **7,** 315 (1953).
5. K. H. Lii, R. C. Haushalter, and C. J. O'Connor, *Angew. Chem. Int. Ed. Eng.* **26,** 546 (1987).
6. R. C. Haushalter and F. W. Lai, *J. Solid State Chem.* **76,** 218 (1988).
7. K. H. Lii and S. L. Wang, *J. Solid State Chem.* **77,** 117 (1988).
8. G. Costentin, M. M. Borel, A. Grandin, A. Leclaire, and B. Raveau, *J. Solid State Chem.* **89,** 31 (1990).
9. N. Kinomura, M. Hirose, N. Kumada, and F. Muto, *Mater. Res. Bull.* **20,** 379 (1985).
10. A. Leclaire, M. M. Borel, A. Grandin, and B. Raveau, *Eur. J. Solid State Inorg. Chem.* **25,** 323 (1988).
11. R. W. G. Wyckoff, "Crystal Structures," Vol. 3, p. 428. Interscience, New York, 1965.
12. R. D. Shannon and C. T. Prewitt, *Acta Crystallogr. Sect. B* **25,** 925 (1969).
13. Z. S. Teweldemedhin, K. V. Ramanujachary, and M. Greenblatt, *Mater. Res. Bull.* **28** 427 (1993).
14. J. Laplume, *Onde Electr.* **335,** 113 (1955).
15. D. E. Appleman and K. T. Evans, "LSUCRE. Indexing and Least-squares Refinement of Powder Diffraction Data," NTIS Document No. PB-216188. Univ. U.S. Geological Service, Washington, DC, 1973.
16. M. Chaunac, *Bull. Chem. Soc. Fr.*, 424 (1971).
17. V. C. Farmer, "The Infrared Spectra of Minerals," Mineralogical Soc., London, 1974.
18. A. Rulmont, R. Cahay, M. Liegeois-Duyckaerts, and P. Tarte, *Eur. J. Solid State Inorg. Chem.* **28,** 207 (1991).
19. C. H. Huang, U. Knop, D. A. Othen, F. W. D. Woodhams, and R. A. Howie, *Can. J. Chem.* **53,** 79 (1975).
20. A. N. Lazarev, "Vibrational Spectra and Structure of Silicates," English translation, Consultants Bureau, New York, 1972.
21. G. R. Levi and G. Peyronel, *Z. Kristallogr. A* **92,** 190 (1935).
22. E. Tillmann, W. Gebert, and W. H. Baur, *J. Solid State Chem.* **7,** 69 (1973).
23. H. McD. McGeachin, *Acta Crystallogr.* **14,** 1286 (1961).
24. J. P. Giroult, M. Goreaud, Ph. Labbé, J. Provost, and B. Raveau, *Mater. Res. Bull.* **16,** 811 (1981).
25. T. M. Dunn, *Trans. Farad. Soc.* **57,** 1441 (1961).
26. L. E. Conroy and M. J. Sienko, *J. Am. Chem. Soc.* **74,** 3520 (1952).
27. R. L. Carlin, "Magnetochemistry," Springer-Verlag, Berlin, 1986.
28. R. L. Carlin, C. J. O'Connor, and S. N. Bathia, *Inorg. Chem.* **15,** 985 (1976).
29. L. Lezama, K. S. Suh, G. Villeneuve, and T. Rojo, *Solid State Commun.* **76,** 449 (1990).
30. L. Lezama, J. M. Rojo, J. L. Pizarro, M. I. Arriortua, and T. Rojo, *Solid State Ionics,* **63–65,** 657 (1993).
31. Z. S. Teweldemedhin, K. V. Ramanujachary, and M. Greenblatt, *J. Solid State Chem.* **95,** 21 (1991).